16th World Conference on Earthquake, 16WCEE 2017

Santiago Chile, January 9th to 13th 2017

Paper N° 1491

Registration Code: S-W1461912262

EARTHQUAKE SCENARIOS FOR SCHOOL BUILDINGS IN THE CITY OF BASEL (SWITZERLAND)

C. Michel[(1)], P. Hannewald[(2)], P. Lestuzzi[(3)], D. Fäh[(4)], S. Husen[(5)], M. Roth[(6)]

[(1)] *Senior researcher, Swiss Seismological Service, ETH Zurich, clotaire@sed.ethz.ch*
[(2)] *Engineer, Résonance Ingénieurs Conseils, Geneva, pia.hannewald@resonance.ch*
[(3)] *Lecturer, Applied Computing and Mechanics Laboratory, EPF Lausanne, pierino.lestuzzi@epfl.ch*
[(4)] *Professor, Swiss Seismological Service, ETH Zurich, faeh@sed.ethz.ch*
[(5)] *Scientist, Cantonal Laboratory, Canton Basel-Stadt, stephan.husen@bs.ch*
[(6)] *Director, Cantonal Crisis Organization, Canton Basel-Stadt, Martin.Roth@jsd.bs.ch*

Abstract

Developing earthquake scenarios for cities in areas with a moderate seismicity is a challenge due to the limited amount of available seismological and engineering data, which is a source of large uncertainties. This concerns both the seismic hazard, for which only recordings for small earthquakes are available and the unknown earthquake resistance of pre-code structures that constitute the vast majority of the building stock. Within the framework of the risk mitigation project of the city of Basel, a pilot study has been performed to estimate the impact and consequences of strong earthquakes of different sizes and return periods on school buildings.

The hazard analysis benefitted from the new Swiss Probabilistic Seismic Hazard Model of 2015 computed for a well-defined reference rock velocity profile. The city of Basel is located in the Rhinegraben, where sedimentary deposits of several hundred meters thickness substantially influence the ground motion. This ground motion amplification has been estimated at high spatial resolution using different methods, including recordings of small events on a dense strong motion network. This estimation benefitted from 20 years of geophysical investigations and a large number of numerical simulations of earthquake ground motion from strong events.

A selection of 121 cantonal school buildings in Basel have been classified according to a specifically developed typology. Most of them are unreinforced masonry or reinforced concrete shear-wall buildings. Displacement-based analyses have been performed to calculate capacity curves representing the behavior of the different types. Based on these capacity curves, fragility and vulnerability curves were derived with new methods with a special attention paid to the uncertainties and their propagation. The fragility curves have been checked against empirical curves to ensure that the analysis method yielded realistic results and further improved.

The scenarios considered in the study are based on historical events, in particular the 1356 Basel event (Mw=6.6), and on the de-aggregation of the Swiss Seismic Hazard Model for 475 years return period. The computations were run with the Openquake software, propagating all the recognized uncertainties. The scenarios allow us to quantify the number of casualties, the number of pupils that cannot go to school and financial losses that such events would cause.

Moreover, a long-term retrofitting project is currently implemented for the school buildings, not only related to earthquake safety. A building type is assigned to the building before and after the retrofit, and a cost-benefit analysis is performed to determine the impact of the retrofitting on the earthquake safety. A framework for real-time assessment is also developed, and a prototype Shakemap at high spatial resolution was implemented as test version.

Keywords: seismic risk; seismic vulnerability; fragility curves; displacement-based assessment; Openquake

1. Introduction

Earthquake scenarios, i.e. estimation of monetary and human losses due to particular earthquakes, are an important tool for decision makers to design appropriate measures to face an event, to quantify the financial consequences of earthquakes and to evaluate the impact of mitigation measures.

Most of the earthquake scenarios produced worldwide at the scale of a city are based on empirical methods (based on macroseismic intensity). Mechanical-based loss assessment has been developed in the frame of the HAZUS software at the end of the 1990s [1]. The Risk-UE project adapted these methods to the European context [2]. However, they are generally based on simplified design structural models and standard design hazard spectra that are hardly compatible with a probabilistic analysis necessary for risk assessment.

Contrarily to the other existing software, Openquake [3] developed by the Global Earthquake Model does not stick to a single vulnerability assessment method since it uses as input any user-developed fragility curve. It is also flexible regarding the hazard data and allows to use the most up-to-date Ground Motion Prediction Equations (GMPEs). The drawback is that the user has to develop himself a comprehensive hazard and vulnerability model. A critical point is that these models have to be consistent with respect to the parameters used and their level of uncertainty: the quality of a prediction depends only on the quality of the most uncertain element in the model ("principle of consistent crudeness" [4]).

The goal of our study is to produce earthquake loss scenarios using the most up to date hazard and engineering models and data within a coherent mechanical-based and probabilistic framework. Probabilistic means that the inputs of the scenarios are considered as uncertain and the whole distribution of expected losses is computed by combining all the uncertainties, aleatory and epistemic. It ensures robustness to the results, points out the elements with the largest uncertainties and evaluates the final uncertainties on the results. Although this is commonly achieved in hazard assessment, this is a remarkable step forward for loss computations. Mechanical-based means that the intensity measures used are physical quantities that can be measured by instruments such as spectral acceleration and not macroseismic intensity. They ensure a better control on physical phenomena to objectively extrapolate models to events that have never been observed in the area of interest.

The present study is focused on the school buildings of the canton Basel-City (Switzerland). It aims at computing the monetary and human losses for different scenario earthquakes, based on historical events and disaggregation of the 2015 Swiss Seismic Hazard Model [5]. Another goal is the estimation of the benefit of the retrofitting measures undertaken by the authorities in the frame of a long-term reorganization project for schools.

Three major scientific targets have been addressed in our study to improve the loss assessment results at the city-scale: comprehensive consideration of uncertainties, reliable ground-motion amplifications for the whole city and realistic vulnerability models. This paper presents the general framework of the scenario computation using Openquake software, the ground-motion computations, the vulnerability of the school buildings and details the results for selected scenarios before and after retrofitting. Subsequent conclusions for the earthquake safety are discussed as well. A more detailed version of this study can be found in [6].

2. Framework

In this study, we are using the Openquake software [3] that provides state of the art tools for seismic risk computation. Moreover, the recent Swiss Seismic Hazard Model 2015 is using Openquake and therefore made the specific models and data for Switzerland available in the software. Openquake is designed for mechanical-based methods and based on ground motion prediction equations and fragility/vulnerability curves that should be function of the predicted Intensity Measure (IM). This framework imposes an extensive work of data selection and pre-processing. However, within this framework, a comprehensive treatment of the uncertainties can be done.

In Openquake, hazard and vulnerability computations are decoupled. For scenario and risk computations, hazard is represented by a set of Ground Motion Fields (GMFs). A GMF is a set of sites (latitude/longitude), for which an

IM value is provided. GMFs may group sets of sites with different Intensity Measures (e.g. PGA, SA(1s) etc.). A large number of GMFs is used to sample the uncertainty in the ground motion (aleatory and epistemic). The losses are computed using the fragility and vulnerability curves for each of the GMF (Monte Carlo sampling) to retrieve the probabilistic losses. The uncertainty in the vulnerability should therefore be fully included in the fragility and vulnerability curves.

Additional features were developed specifically for the study, especially the derivation of fragility and vulnerability curves. Another important additional feature was the inclusion of site amplification. The general workflow of the computation is displayed in Fig. 1.

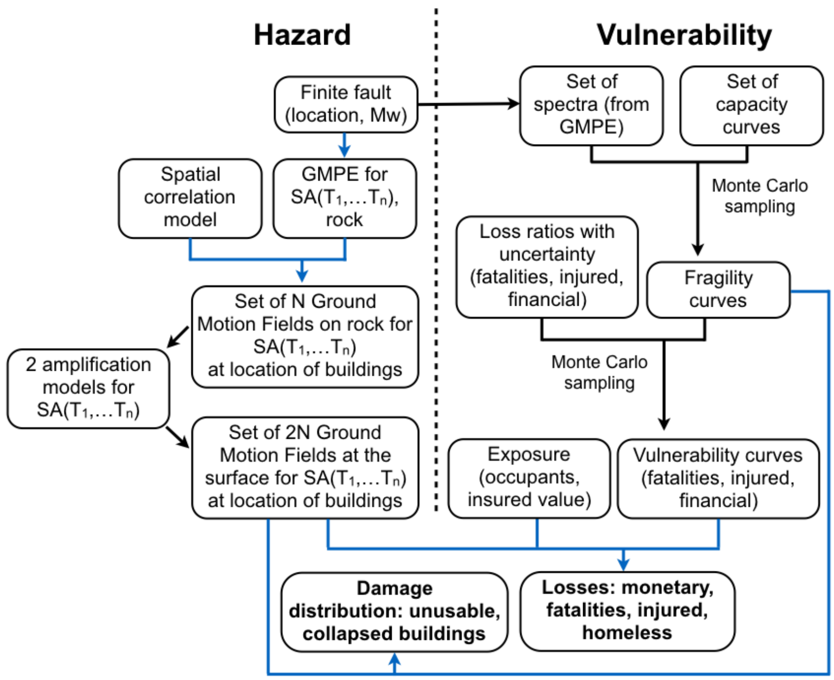

Fig. 1 – Workflow of the scenario computation. Blue arrows denote computations performed using Openquake.

3. Ground motion scenarios in Basel

3.1 Scenarios

The scenario earthquakes have been selected out of the historical damaging events in Basel and the disaggregation of the Swiss Seismic Hazard model 2015 [5].

Basel's strongest historical earthquake, constituting our first scenario, is the Mw=6.6 event that occurred on October 18th 1356 [7]. It destroyed the city and caused damage in many villages around, though the number of fatalities remained limited [7]. Ferry et al. [8] reconstructed sections of the Reinach fault that may have ruptured in 1356 (in blue in Fig. 2). The Northern and Southern ends of the ruptured fault are uncertain. However, it is located so close to the city that the distance between the buildings and the rupture is nearly the assumed depth (2 km assumed here).

The Swiss Hazard Model 2015 [5] used all the available seismicity information and the most up to date ground motion prediction models to estimate the probability of occurrence of each ground motion intensity measures (PGA and Spectral Acceleration) for the theoretical Swiss reference-rock model [9]. It is also providing the disaggregation of the results for a given probability value. We consider here the probability of occurrence of 10% in 50 years, corresponding to a return period of 475 years. For this particular value, the PGA value is 0.085 g in Basel at the reference rock. The most likely value of the distribution of the events contributing to this estimated

PGA corresponds to an event of magnitude Mw of 5.6 to 5.7 located at 5 to 10 km distance. Therefore, we selected a scenario of Mw=5.7 located on a fault oriented parallel to the Reinach fault at a distance of 7.5 km of the buildings of interest and with a length compatible with the size of the event (orange line in Fig. 2).

Within the distribution of the disaggregation results, we picked up an event of Mw=5.0 at 5 km distance (green color in Fig. 2) that we used as another possible scenario.

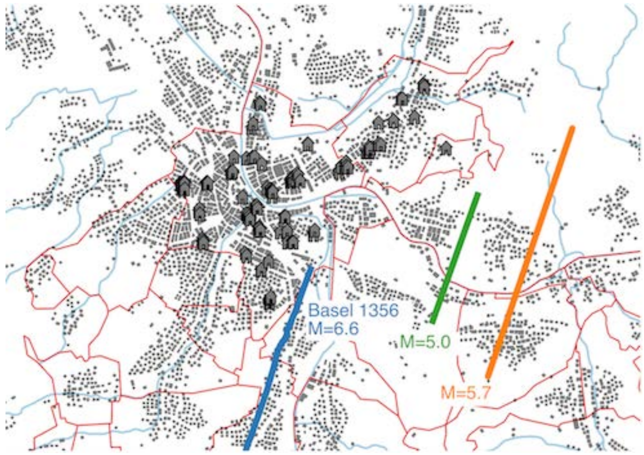

Fig. 2 – Surface trace of the faults used for the different scenarios. The considered school buildings are displayed.

3.2 Ground motion prediction

The Swiss Stochastic Model developed by Edwards and Fäh [10] and parameterized by Cauzzi et al. [11] is the most appropriate Ground Motion Prediction model (GMPE) available for the considered area. It is based on the analysis of the recorded events in Switzerland and a physics-based model. The predicted ground motion corresponds to the Swiss Reference Rock model [9] with Vs_{30}=1100 m/s and corresponds approximately to the weathered Molasse rock of the Swiss Foreland. It provides the aleatory uncertainties in terms of single-station sigma so that the uncertainties related to the site response can be accounted for separately.

The stress drop is also an input parameter of the model and has been chosen as 60 bars as recommended by Cauzzi et al. [11] who validated this value with the events in the Swiss historical catalog.

Weatherill et al. [12] showed that the spatial correlation in the variability of the GMPEs was important for the results of loss scenarios. It does not affect the mean value of ground motion and damage at each site but the uncertainties when losses at different sites are aggregated. Although spatial correlation is a property of the GMPE, the existing spatial correlation models are not significantly different [13]. Therefore, we used the model of Jayaram and Baker [14], available in Openquake, to generate spatial correlation in the GMFs.

3.3 Ground motion amplification [15]

The largest part of the city of Basel is located in the Rhine Graben where deep Tertiary and Quaternary sediments exist (up to 1000 m depth). These sediments are partly consolidated with a Vs_{30} value around 400-500 m/s and lead to a significant amplification of the ground motion (around a factor of 3 with respect to the Swiss reference rock). We reviewed and improved the mapping of the amplification in the Basel area in terms of spectral acceleration. We proposed two alternative amplification maps that have been used for the scenario computation: a map based on the microzonation proposed in 2006 [16] corrected to the reference rock model and a new map based on the interpolation of the observed amplification at the Swiss Strong Motion Network computed following Edwards et al. [17].

We treated differently the Rhine Graben and its deep sediments and the area outside of the Graben where Quaternary sediments with variable thicknesses (<35 m) and quality lay directly on Mesozoic rock. The considered portfolio of school buildings is mainly located in the Rhine Graben where the amplification is rather

homogeneous. Two school buildings are located outside of the Graben and are both equipped with a modern strong motion station, for which Edwards et al. [17] directly provide the amplification function.
We computed 500 GMFs for each amplification model yielding a total of 1’000 GMFs.

4. Vulnerability of Basel school buildings

4.1 Taxonomy

The present study focuses on cantonal schools in Basel City. Out of the 250 structures constituting the building stock, only the 121 buildings with classrooms were selected for the study. The considered elements at risk are therefore the individual school buildings, associated to a building type, a replacement cost and a number of pupils. For the project we assumed full occupancy, corresponding to an event occurring during school hours.
Information on each structure was collected based on the archive of the buildings department, some recent engineering reports and visits. In the frame of a project of change in the education system, the cantonal building department decided to systematically assess all schools built prior to the publication of the first seismic design code in Switzerland in 1989 and to retrofit where necessary. Hence, two scenarios are considered here: before and after retrofitting.
The oldest school has been built in the 15^{th} century and the majority in the 20^{th} century but more than three quarters of the schools were built before 1989 and only a rather small percentage was designed according to nowadays codes. Most of the schools are reinforced concrete and masonry or mixed structures, although some lightweight structures are also present. Based on the available information, buildings were grouped according to their characteristics, and primarily their construction material as usually done (e.g. [17]).
Masonry structures (M) were subdivided in two groups: L light masonry (modern bricks with voids) and H heavy masonry (stone masonry and solid bricks). A further refinement of masonry building classes has been made according to the floor type: RF rigid floor (concrete slabs, hourdis), FF flexible floor (wooden floor).
Reinforced concrete buildings (RC) were first categorized according to the type of load bearing structure as follows: W wall structures, F frame structures, FW frames in one direction and walls in the other and P particularities, such as buildings with an irregular mixed wall and frame structure and post-tensioned concrete structures. Furthermore, as the behavior of squat and slender wall structures is different, the category W was refined into: S slender walls with an aspect ratio greater than 1.5 and NS non-slender walls with an aspect ratio equal to or smaller than 1.5
Mixed structures eventually turned out to be RC frames with masonry infill (MI). Two types of potentially vulnerable elements were identified: masonry walls that do not span the entire height of the frame and frames that are infilled in all but a single story. The first type of element is vulnerable to out-of-plane (OOP) failure and, under in-plane loading, the RC columns may develop a short column effect. The second type is prone to develop a soft story mechanism (SS).
The type Others (OTH) comprises all buildings that could not be attributed to any other class; a lot of them lightweight structures, presumably made of relatively small wood or sandwich panels.
The difference between the scenarios before and after retrofitting is the attribution of buildings to different types rather than a change in the models for each type. 33 schools were retrofitted in such a way that their type changed after retrofitting (all retrofitting measures could not be mapped with a change of type).

Table 1 –Typology and distribution of buildings before (BR) and after (AR) retrofitting.

Types				Number BR	Number AR
M: Masonry	H: Heavy (Stone, solid bricks)	FF: Flexible Floors	M_H_FF	25	9
		RF: Rigid Floors	M_H_RF	6	22
	L: Light (hollow bricks)	FF: Flexible Floors	M_L_FF	2	1
		RF: Rigid Floors	M_L_RF	10	9
RC: Reinforced-Concrete	F: Frames		RC_F	10	6
	W: Walls	S: Slender walls	RC_W_S	17	23
		NS: Non-Slender walls	RC_W_NS	8	16
	FW: Frames and Walls		RC_FW	10	12
	P: Particular		RC_P	3	1
MRC: Masonry and Reinforced Concrete	MI: Masonry Infill	OOP: Out-Of-Plane	MRC_MI_OOP	12	5
		SS: Soft-Story	MRC_MI_SS	2	1
OTH: Others			OTH	16	16

4.2 Fragility curves

We associated each type to a structural model following a non-linear static procedure assuming a single-degree-of-freedom system. Each type is represented by a bilinear capacity curve defined by 3 parameters: the elastic period T, the yield displacement d_y and the ultimate displacement d_u. For each building type, one to three typical buildings were modelled using adequate 2D models in order to generate capacity curves. Input parameters were chosen based on the latest available laboratory tests. Besides, the elastic period has been further validated in the project by ambient vibration measurements in buildings as proposed by Michel et al. [19,20,21]. Finally, stochastic sets of capacity curves were computed based on intervals in the values of the input parameter for each model.

The EMS98 damage scale is used in this project [22]. It has 5 grades: slight, moderate, severe, partial collapse and complete collapse, defined from the description of building damage. The corresponding limit states of the model have been defined in terms of displacement capacity from the capacity curves. DG1 corresponds to a displacement exceeding $0.7*d_y$, DG2 to $1.5*d_y$, DG3 to $½*(1.5*d_y+d_u)$ and DG4 to d_u (based on [18]). The fifth damage grade is estimated based on the assumption that the damage grades follow a binomial distribution, as proposed in [17].

For each level of ground motion, the response of the set of capacity curves to a set of spectra derived from the Akkar et al. [23] ground motion prediction equation, conditioned on the selected ground motion value, is computed using the Lin and Miranda [24] method. This GMPE was used because Akkar et al. [25] provide the inter-period correlation matrix, needed for this computation. The distribution of the damage grades reached for these computations constitute the fragility curves. They are defined discretely, without fitting a lognormal distribution. The set of spectra used depend on the chosen scenario in the GMPE (magnitude, distance, style of faulting and Vs_{30}) so that the fragility curves are as well scenario-dependent.

They include: 1) aleatory uncertainties due to the different characteristics of the buildings constituting a type and the variability in the response to a ground motion level defined by a single parameter and 2) epistemic uncertainties due to assumptions chosen in the modelling. As a result, uncertainties increase with the level of ground motion, deviating from the lognormal assumption. However, epistemic uncertainties may still be underestimated and their evaluation would require the use of more advanced models.

Furthermore, the obtained fragility curves were compared to empirical curves and the base assumptions of the structural models were eventually revised in order to avoid using conservative models.

4.4 Loss ratios and vulnerability curves

In order to derive vulnerability curves, i.e. the probabilistic distribution of loss ratios (fatalities, injured and financial) as a function of the chosen IM, fragility curves are combined with loss ratios. Each DG corresponds to a probabilistic distribution of loss ratios. In this project, loss ratios are assumed to follow a uniform distribution between two plausible bounds obtained from the literature. The combination of fragility curves and loss ratios is performed by Monte Carlo analysis: a large number of random samples in the damage distribution (as defined by the fragility curves) are multiplied by (independent) random values from the loss ratio distribution in order to determine the distribution of the losses.

The so-called lethality rates were defined “as the ratio of the number of people killed to the number of occupants present in collapsed buildings of that class” [26]. Based on this concept, casualty models have been proposed in the literature for different countries and calibrated with observed data. Although more detailed models exist, we consider only 2 levels of casualty here: injury needing medical aid (including slight injuries) and death. Since only structural collapse is considered, only DG4 and 5 EMS98 are generally associated to casualty ratios, though collapse of non-structural elements, occurring at DG1-3 can also be associated to injuries or even deaths. We selected the casualty ratios for the different building types based on FEMA [27], Spence [28] complemented by So and Spence [29], Zuccaro and Cacace [30] and Jaiswal et al. [31].

In order to estimate the property loss, one uses the repair cost ratio, defined as the ratio between the cost of repair and the replacement cost. The studies of Kircher et al. [32], D’Ayala et al. [33], Tyagunov et al. [34] and Silva et al. [35] have been compared to retrieve loss ratios (minimum and maximum value).

5. Results

5.1 Ground motion fields

The amplitude of the retrieved median ground motion field is logically strongly increasing with magnitude. SA(1s), corresponding to tall flexible buildings (RC_P and MRC_MI_SS in our scenarios) is amplified in the Rhine Graben, while larger values of SA(0.3s) are noticed outside of the Graben. Such interaction between source, site and building can only be reproduced when mechanical scenarios are used, not empirical ones. The median ground motion does however not correspond to a realistic spatial distribution of ground motion: Fig. 3 shows examples of ground motion fields with full correlation and with a spatial correlation model. Full correlation (median ground motion here) allows to clearly define the level of ground motion, while the spatial correlation model provide more realistic fields although one can then hardly recognize a ground motion “level”. If one converts the ground motion fields into macroseismic intensity following Faenza and Michellini [36], the intensity produced by the scenario Mw=6.6, 5.7 and 5.0 are 8.9, 7.7 and 7.0 in the city center.

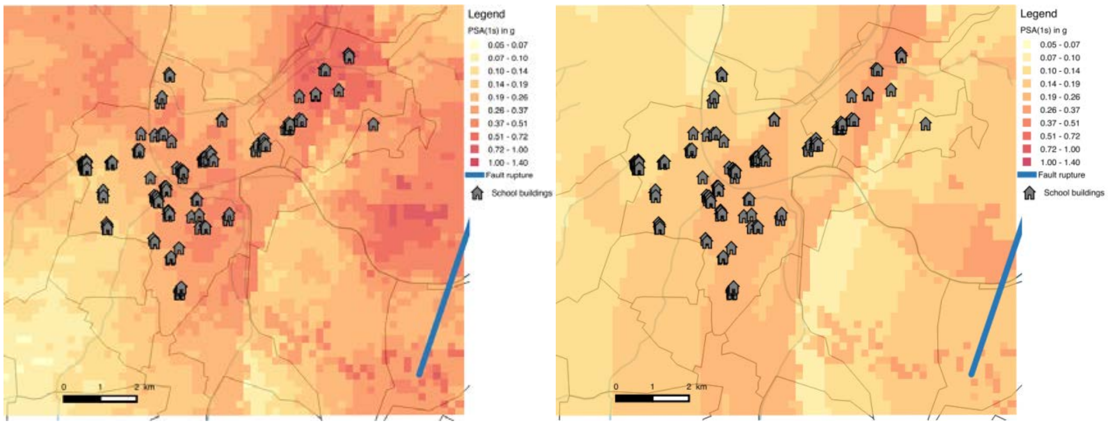

Fig. 3 – Effect of spatial correlation on ground motion: example ground motion fields PSA(1s) with (left) and without (right) spatial correlation for the Mw=5.7 scenario event. The right GMF corresponds to the median GMF.

5.2 Losses

Table 2 summarizes the results of the 3 investigated scenarios, after the retrofitting project. An event similar to the 1356 earthquake would be a catastrophe: nearly all school buildings would be unusable and a large number of fatalities (several hundreds) and injured would be resulting. In the two scenarios from the deaggregation, ten (M=5) or several tens (M=5.7) of fatalities may still occur, but building collapse, even partial, is not certain. The uncertainties, mostly driven by the uncertainties in the GMPE, are nearly as large as the mean values so that only the order of magnitude should be considered. A large part of the building stock would however not be usable right after the event.

As a comparison, during the 2009 L'Aquila (Mw=6.3) event, about 4% of the 1665 buildings surveyed by Tertulliani et al. [37] in the city completely collapsed (DG5), 20% suffered at least partial collapse (DG≥4) and 90% were not usable (DG≥2). Given the magnitude and distance to the city, intermediate between our 1356 and the M=5.7 scenario, our results are therefore coherent.

Large numbers of victims logically occur in the most vulnerable building types with a large number of pupils. The large majority of fatalities occur in masonry buildings (about 70% for the 1356 and 5.7 scenarios). The share of the financial losses in masonry structures is lower but still dominant (about 60%).

For a given scenario, ground motion is relatively homogeneous over the considered area (most of the schools are in the Rhine Graben) so that site effects do not explain much of the spatial variability in the losses.

It is also important to notice that the mean damage grades are low for all the buildings. For the M=5.7 scenario, the mean damage grade does not exceed 2.6, that is to say, on average, they are not expected to collapse and to induce fatalities. Deterministic approaches would only consider this parameter and would therefore fail predicting fatalities.

The results are particularly sensitive to the choice of the GMPE, easily changing the results by a factor of 2. The site effects play an important role (they increase the losses by a factor of 3), but their uncertainty in this case has been strongly reduced by the large amount of data and models gathered in previous works. Moreover, the choice of the Intensity Measure(s) is also critical for the results and related uncertainties.

Table 2 –Results from the scenarios after retrofitting

	Basel 1356	**M=5.7@7.5km**	**M=5@5km**
Out of **121** buildings			
not usable (DG≥2)	102±48 (**84%**)	61±50 (**50%**)	44±39 (**36%**)
At least partial collapse (DG≥4)	35±6 (**29%**)	6±3 (**5%**)	2±2 (**2%**)
Total collapse (DG5)	12±4 (**10%**)	1±1 (**1%**)	0±1 (**<1%**)
Out of **16960** pupils			
Fatalities	305±130 (**2%**)	33±30 (<**1%**)	10±13 (<**1%**)
Injured	1814±709 (**11%**)	242±189 (**1%**)	88±82 (**1%**)
Homeless (DG≥2)	13129 (**77%**)	8809 (**52%**)	6311 (**37%**)
Total value **1143 MCHF**			
Total losses (MCHF)	566±122 (**50%**)	210±94 (**18%**)	126±49 (**11%**)

5.3 Cost-benefit analysis of the retrofitting

The differences between the results before and after retrofitting are relatively limited when compared to the uncertainties, but they are considerable in absolute value. The difference before/after retrofitting is computed in Tab. 3 for the 33 buildings out of 121 that have been or are planned to be retrofitted. Victims are approximately divided by 2 for all the events. The financial gain is smaller, around 25%. It corresponds to direct losses of 13 MCHF for the 475 yrs. return period event with Mw of 5.7. This number could be compared to the investment of the city in the seismic retrofitting of the 33 buildings.
The retrofitting measures are in general limited and target the loss of life that is indeed improved.

Table 3 –Loss gain between before and after retrofitting for the 33 retrofitted buildings only

	Basel 1356	**M=5.7@7.5km**	**M=5@5km**
Fatalities	46%	62%	59%
Injured	43%	54%	48%
Total losses	23%	25%	24%

6. Conclusions

In this study, we computed loss scenarios in the city of Basel based on mechanical approaches. A comprehensive estimation of the uncertainties has been performed and will allow to better understand the sources of uncertainty.

The performed scenarios are more precise and robust than previous studies through the coherent combination of the most up to date hazard and vulnerability data and models including their uncertainties. We showed that the later are large, in the same order of magnitude as the mean values. In the future, the uncertainty in each individual part of the computation has to be decreased to improve the results.

During the development of the fragility curves, we observed that currently used seismic analysis methods were too conservative, *i.e.* biased towards higher vulnerability, to be directly used for risk scenarios and that conservativeness needed to be first removed.

We performed a number of selected damage scenarios on the school buildings of Basel and evaluated for each the distribution of damage, the number of fatalities, injured and homeless pupils and the financial losses. Although total collapse of a school building is not certain for the 475 yrs. return period event (M=5.7), tens of fatalities should be expected as well as large financial losses. A large amount of the buildings would be moderately damaged, meaning that they would need a quick analysis and repair, which can be challenging considering the large amount of affected structures and the limited number of trained engineers for such cases.

Despite the large uncertainties, we showed that the retrofitting measures had a noticeable impact on the results (50% less fatalities for the group of retrofitted buildings). The strategy of retrofitting with a priority on the weakest structures with the largest number of occupants is proven to be efficient. However, retrofitting does not mean reducing the losses to 0, even for the scenario with 475 yrs. return-period. A more detailed analysis on the retrofitted buildings is however necessary to be able to precise this statement.

The results are obviously very different depending on the scenario itself (magnitude, distance …), but this information could be obtained shortly after an earthquake and the scenarios computed in near real-time. This model is therefore a solid basis for extending loss scenarios to the whole city and in real-time.

7. Acknowledgements

This project “Earthquake mitigation of Canton Basel-Stadt (2013-2016)” has been funded by the Canton Basel-Stadt.

8. References

[1] Kircher CA., Whitman RV, Holmes WT (2006): HAZUS Earthquake Loss Estimation Methods. *Nat. Hazards Rev.* **7**, 45–59.

[2] Mouroux P, Le Brun B (2006): Presentation of RISK-UE project. *Bull. Earthq. Eng.* **4**, 323–339.

[3] Silva V, Crowley H, Pagani M, Monelli D, Pinho R (2014): Development of the OpenQuake engine, the Global Earthquake Model’s open-source software for seismic risk assessment. *Nat. Hazards* **72**, 1409–1427.

[4] Elms DG (1985): Principle of Consistent Crudeness, *Workshop on Civil Engineering Applications of Fuzzy Sets*, Purdue University, West Lafayette, Indiana, USA.

[5] Wiemer S and the Hazard team of the Swiss Seismological Service (2015): Swiss National Probabilistic Seismic Hazard Assessment 2015. Zurich, Switzerland.

[6] Michel C, Hannewald P, Lestuzzi P, Fäh D, Husen S (2016): Probabilistic mechanics-based loss scenarios for school buildings in Basel (Switzerland). *Bull. Earthq Eng*. doi: 10.1007/s10518-016-0025-2

[7] Fäh D, Gisler M, Jaggi B, Kästli P, Lutz T, Masciadri V, Matt C, Mayer-Rosa D, Rippmann D, Schwarz-Zanetti G, Tauber J, Wenk T (2009): The 1356 Basel earthquake: an interdisciplinary revision. *Geophys. J. Int.* **178**, 351–374.

[8] Ferry M, Meghraoui M, Delouis B, Giardini D (2005): Evidence for Holocene palaeoseismicity along the Basel-Reinach active normal fault (Switzerland): A Seismic source for the 1356 earthquake in the Upper Rhine graben. *Geophys. J. Int.* **160**, 554–572.

[9] Poggi V, Edwards B, Fäh D (2011): Derivation of a Reference Shear-Wave Velocity Model from Empirical Site Amplification. *Bull. Seismol. Soc. Am.* **101**, 258–274.

[10] Edwards B, Fäh D (2013): A Stochastic Ground-Motion Model for Switzerland. *Bull. Seismol. Soc. Am.* **103**, 78–98.

[11] Cauzzi C, Edwards B, Fäh D, Clinton J, Wiemer S, Kastli P, Cua G, Giardini D (2015): New predictive equations and site amplification estimates for the next-generation Swiss ShakeMaps. *Geophys. J. Int.*, **200**, 421–438.

[12] Weatherill GA, Silva V, Crowley H, Bazzurro P (2015): Exploring the impact of spatial correlations and uncertainties for portfolio analysis in probabilistic seismic loss estimation. *Bull. Earthq. Eng.* **13**(4), 957-981.

[13] Esposito S, Iervolino I (2012): Spatial Correlation of Spectral Acceleration in European Data. *Bull. Seismol. Soc. Am.* **102**, 2781–2788.

[14] Jayaram N, Baker JW (2009): Correlation model for spatially distributed ground-motion intensities. *Earthq. Eng. Struct. Dyn.* **38**, 1687–1708.

[15] Michel C, Fäh D, Edwards B, Cauzzi C (2016) : Site amplification at the city scale in Basel (Switzerland) from geophysical site characterization and spectral modelling of recorded earthquakes. *Physics and Chemistry of the Earth, Parts A/B/C*. http://doi.org/10.1016/j.pce.2016.07.005

[16] Fäh D, Wenk T (2009): Mikrozonierung für die Kantone Basel Stadt und Basel Landschaft. Optimierung der Form der Antwortspektren und der Anzahl der Mikrozonen. *Abschlussbericht : Teilbericht B.*, Zurich, Switzerland.

[17] Edwards B, Michel C, Poggi V, Fäh D (2013): Determination of Site Amplification from Regional Seismicity: Application to the Swiss National Seismic Networks. *Seismol. Res. Lett.* **84**, 611–621.

[18] Lagomarsino S, Giovinazzi S (2006): Macroseismic and mechanical models for the vulnerability and damage assessment of current buildings. *Bull. Earthq. Eng.* **4**, 415–443.

[19] Michel C, Guéguen P, Causse M (2012): Seismic vulnerability assessment to slight damage based on experimental modal parameters. *Earthq. Eng. Struct. Dyn.* **41**, 81–98.

[20] Michel C, Guéguen P, Lestuzzi P, Bard PY (2010): Comparison between seismic vulnerability models and experimental dynamic properties of existing buildings in France. *Bull. Earthq. Eng.* **8**, 1295–1307.

[21] Michel C, Zapico B, Lestuzzi P, Molina FJ, Weber F (2011): Quantification of fundamental frequency drop for unreinforced masonry buildings from dynamic tests. *Earthq. Eng. Struct. Dyn.* **40**, 1283–1296.

[22] Grünthal G, Musson RMW, Schwartz J, Stucchi M (1998): European Macroseismic Scale 1998. *Cahiers du Centre Européen de Géodynamique et de Séismologie*, Luxembourg.

[23] Akkar, S., Sandikkaya, M. a. & Bommer, J. J. Empirical ground-motion models for point- and extended-source crustal earthquake scenarios in Europe and the Middle East. *Bull. Earthq. Eng.* **12,** 359–387 (2014).

[24] Lin Y, Miranda E (2008): Noniterative Equivalent Linear Method for Evaluation of Existing Structures. *J. Struct. Eng.* **134**, 1685–1695.

[25] Akkar S, Sandikkaya MA, Ay BO (2014): Compatible ground-motion prediction equations for damping scaling factors and vertical-to-horizontal spectral amplitude ratios for the broader Europe region. *Bull. Earthq. Eng.*, **12**, 517–547.

[26] Coburn A, Spence R, Pomonis A (1992): Factors determining human casualty levels in earthquakes: mortality prediction in building collapse. *10th World Conference of Earthquake Engineering (WCEE)*, Madrid, Spain.

[27] FEMA (2012): Multi-hazard loss estimation methodology: earthquake model. Hazus–MH 2.1: *Technical Manual*.

[28] Spence R (2007): LESSLOSS Report 2007/07 - Earthquake Disaster Scenario Predictions & Loss Modelling for Urban Areas, IUSS Press.

[29] So E, Spence R (2013): Estimating shaking-induced casualties and building damage for global earthquake events: A proposed modelling approach. *Bull. Earthq. Eng.* **11**, 347–363.

[30] Zuccaro G, Cacace F (2011): Seismic Casualty Evaluation: The Italian Model, an Application to the L’Aquila 2009 Event, *in: Spence, R., So, E., Scawthorn, C. (Eds.), Human Casualties in Earthquakes*. Springer, 171–184.

[31] Jaiswal K, Wald DJ, Earle PS, Porter KA, Hearne M (2011): Earthquake Casualty Models Within the USGS Prompt Assessment of Global Earthquakes for Response (PAGER) System, *Human Casualties in Earthquakes*. 83–94.

[32] Kircher CA., Reitherman RK, Whitman RV, Arnold C (1997): Estimation of earthquake losses to buildings. *Earthq. Spectra* **13**, 703–720.

[33] D’Ayala D, Spence R, Oliveira CS, Pomonis A (1997): Earthquake Loss Estimation for Europe’s Historic Town Centres. *Earthq. Spectra* **13**(4), 773-793.

[34] Tyagunov S, Stempniewski L, Grünthal G, Wahlström R, Zschau J (2004): Vulnerability and Risk Assessment for Earthquake Prone Cities, *13th World Conference on Earthquake Engineering*, Vancouver, Canada.

[35] Silva V, Crowley H, Varum H, Pinho R (2015): Seismic risk assessment for mainland Portugal. *Bull. Earthq. Eng.* **13**, 429–457.

[36] Faenza, L. & Michelini, A. Regression analysis of MCS intensity and ground motion spectral accelerations (SAs) in Italy. *Geophys. J. Int.* **186,** 1415–1430 (2011).

[37] Tertulliani A, Arcoraci L, Berardi M, Bernardini F, Camassi R, Castellano C, Del Mese S, Ercolani E, Graziani L, Leschiutta I, Rossi A, Vecchi M (2010): An application of EMS98 in a medium-sized city: The case of L'Aquila (Central Italy) after the April 6, 2009 Mw 6.3 earthquake. *Bull. Earthq. Eng.* **9**, 67–80.